AIMS Mathematics, 9(6): 13589–13606.
DOI: 10.3934/math.2024663
Received: 12 January 2024
Revised: 26 March 2024
Accepted: 27 March 2024
Published: 12 April 2024

http://www.aimspress.com/journal/Math

Research article

Analytical insights into solitary wave solutions of the fractional Estevez-Mansfield-Clarkson equation

M. Mossa Al-Sawalha[1], Saima Noor[2,3,*], Saleh Alshammari[1], Abdul Hamid Ganie[4] and Ahmad Shafee[5]

[1] Department of Mathematics, College of Science, University of Ha'il, Ha'il 2440, Saudi Arabia

[2] Department of Basic Sciences, Preparatory Year, King Faisal University, Al-Ahsa 31982, Saudi Arabia

[3] Department of Mathematics and Statistics, College of Science, King Faisal University, Al-Ahsa 31982, Saudi Arabia

[4] Basic Science Department, College of Science and Theoretical Studies, Saudi Electronic University, Riyadh 11673, Saudi Arabia

[5] PAAET, College of Technological Studies, Laboratory Technology Department, Shuwaikh 70654, Kuwait

* **Correspondence:** Email: snoor@kfu.edu.sa.

Abstract: This study delved into the dynamics of wave solutions within the Estevez-Mansfield-Clarkson equation in fractional nonlinear space-time. Utilizing conformable fractional derivatives, the equation governing shallow water phenomena and fluid dynamics was transformed into a nonlinear ordinary differential equation. Applying the Riccati Bernoulli sub-ODE approach yielded a finite series representation. Notably, our findings revealed novel solitary wave solutions characterized by kink, anti-kink, periodic, and shock functions. Visualized through 3D and contour graphs, kink and periodic waves emerged as distinct observable manifestations. Intriguingly, the diversity of results surpassed previous results, contributing to a deeper understanding of the intricate dynamics inherent in the system.

Keywords: fractional Estevez-Mansfield-Clarkson (EMC) equation; solitary wave solution; analytical method
Mathematics Subject Classification: 33B15, 34A34, 35A20, 35A22, 44A10

1. Introduction

Nonlinear evolution equations are essential to applied mathematics, applied science, and engineering because of their wide range of practical applications. Many models have drawn a lot of attention, including those related to fluid dynamics, fluid mechanics, neurons, optical fibers, electrical circuits, waves in water, plasma oscillations, capillary-gravity waves, physics of plasma, chemical kinetics, and chemical physics. To gain a greater understanding of the dynamics of these real-world components, methods for solving fractional nonlinear partial differential equations (PDEs) must be investigated. To further study and understand the complex behaviors that are inherent in the aforementioned systems, this exploration is essential. Solutions to fractional nonlinear PDEs are of academic interest because of the increased detail and generality they provide, which outperforms traditional solutions in terms of descriptive power. Additionally, graphs representing the physical solutions of various fractional orders can be compared. To investigate new findings for the exact traveling wave solutions, mathematicians have developed and implemented innovative and reliable techniques. Some of these methods are the Khater II method [1], generalized Khater method [2], modified Khater method [3], simple equation method [4], Poincare-Lighthill-Kuo method [5], generalized Kudryashov method [6], modified Kudryashov method [7], fractional sub-equation method [8] and (G'/G)-expansion method [9]. Recent studies have used a variety of techniques to investigate solutions for solitary waves, revealing a wide range of approaches to comprehending intricate physical phenomena. Scholars have conscientiously employed several techniques, all of which have added significant value to our understanding of the nature and dynamics of isolated waves [10–14]. These joint efforts have improved our knowledge of nonlinear dynamics and provided a wide range of solitary wave solutions, which have enhanced the scientific discourse [15–19].

Numerous mathematical strategies have been developed to solve the difficulties involved in solving fractional partial differential equations (FPDEs) analytically. Through the revelation of the exact behavior of the modeled system, these strategies seek to overcome the inherent complexity of FPDEs and provide benefits over numerical methods. The knowledge obtained from analytical solutions advances our understanding of basic physical processes more thoroughly. As such, the study of analytical solutions in the field of FPDEs is an important and constantly developing field of research [20–24]. The scientific literature demonstrates the wide range of mathematical techniques used to analytically solve FPDEs, highlighting the complexity of the methods used by experts in this area. Interestingly, a range of approaches [25–33] have been included, highlighting their importance in the variety of strategies that are being examined.

Furthermore, within the parameters of the suggested methodology [34–36], which is known for its skillful management of complex algebraic calculations, the extraction of solutions for a wide range of phenomena, such as fluid dynamics and transport phenomena, offers a potential pathway for applications in a variety of scientific and engineering fields. The intended application in biological systems, industrial processes, and environmental flows has the potential to provide insightful knowledge about the complexities of fluid behavior, leading to improved prediction and optimization techniques. The given partial differential equations are converted into an algebraic system of equations by using the Riccati-Bernoulli equation in conjunction with the Backlund transformation. This approach makes it easier to retrieve important information from the complex behaviors these dynamic systems display, which improves our understanding of the underlying physical processes.

Most notably, the method guarantees the derivation of finite solutions, guaranteeing the accuracy and effectiveness of solutions for the examined equations. One important aspect of this method is its ability to produce a wide range of single-wave solutions.

In addition, the current study attempts to apply this analytical approach to clarify the complex dynamics found in the Estevez-Mansfield-Clarkson (EMC) equation. The 1997 study by Mansfield and Clarkson on pattern dispersion in liquid drops provided the basis for this fourth-order nonlinear evolution equation. The EMC equation poses a difficult set of complications and is mostly used to examine wave behavior in shallow water. By putting the suggested technique to use, this study hopes to further our understanding of these complexities and promote improvements in the field of complex phenomenon analysis. The goals that have been mentioned are intended to improve our comprehension of the behavior of the EMC equation and further our collective efforts to address the difficulties presented by very complex mathematical models.

The EMC equation was developed as a result of research into the dispersion patterns found in liquid droplets. This specific equation, which is utilized in the research, is essential for deciphering the complex dynamics of waves in shallow water. The particular form under examination is a fourth-order fractional nonlinear space-time EMC equation, which may be stated as follows [4]:

$$D_y^{3\beta}(D_t^{\alpha}(F)) + \lambda D_y^{\beta}(F) D_t^{\alpha}(D_y^{\beta}(F)) + \lambda D_y^{2\beta}(F) D_t^{\alpha}(F) + D_t^{2\alpha}(F) = 0, \quad 0 < \alpha, \beta \leq 1, \tag{1.1}$$

where $F = F(x, y, t)$ and $(\lambda \neq 0)$ is a constant. The EMC equation is a key equation in the vast field of nonlinear science. It has applications in fluid dynamics, optics, image processing, and plasma physics. The importance of the EMC equation has been highlighted by recent studies [37–39], which highlight how vital it is to comprehending intricate physical processes. For higher-dimensional nonlinear evolution equations, the investigations use novel approaches like the Sine-Gordon expansion method to find steady soliton solutions for non-linear equations that have not been solved before. Furthermore, the dynamics of important equations are investigated, such as the fractional Ablowitz-Kaup-Newell-Segur equation and the non-linear space-time fractional EMC equation. These investigations offer important insights into wave propagation in many scientific fields. Continuing this direction, the studies explore linked sine-Gordon equations and solitary wave solutions for the EMC equation, two essential mathematical models for studying shape development in many physical contexts. All of these discoveries highlight how important the EMC equation is to improve our comprehension of complex systems and how they materialize in the actual world.

The operator that represents the derivatives of order α adheres to the definition provided in [40].

$$D_{\theta}^{\alpha} q(\theta) = \lim_{m \to 0} \frac{q(\theta + m(\theta)^{1-\alpha} - q(\theta))}{m}, \; 0 < \alpha \leq 1. \tag{1.2}$$

2. Methodology

Consider the following fractional partial differential equation (FPDE) that we have presented:

$$P_1\left(f, D_t^{\alpha}(f), D_{\zeta_1}^{\beta}(f), D_{\zeta_2}^{2\beta}(f), f D_{\zeta_1}^{\beta}(f), \ldots\right) = 0, \quad 0 < \alpha, \beta \leq 1. \tag{2.1}$$

Polynomial P_1 is a function of $f(\zeta_1, \zeta_2, \zeta_3, \cdots, t)$. This polynomial includes the fractional order derivatives as well as the nonlinear terms. The primary stages of this method are then thoroughly

covered. The wave transformations that follow are our suggestions for looking into possible solutions for Eq (1.1):

$$F(x, y, t) = e^{i\psi} f(\psi), \tag{2.2}$$

where

$$\psi(x, y, t) = p\left(\frac{x^{\gamma}}{\gamma}\right) + q\left(\frac{y^{\beta}}{\beta}\right) - \omega\left(\frac{t^{\alpha}}{\alpha}\right). \tag{2.3}$$

A universal variable denoting the transformation of propagating waves is represented by the symbol (ψ). Three non-zero constants, (p), (q) and (ω), give different features to the travelling wave dynamics. More specifically, for $\omega > 0$, the wave travels in a positive direction and for $\omega < 0$, the wave travels in a negative direction. We apply a transformation to Eq (2.1) that results in the formation of a nonlinear ordinary differential equation (NODE) and, as a result, assumes a modified mathematical expression. This change reflects an intrinsic change in the nature of the equation, which goes from its original form to a non-linear one. This introduces new dynamics and behaviors, which call for an improved mathematical representation.

$$P_2\left(f, f'(\psi), f''(\psi), ff'(\psi), \ldots\right) = 0. \tag{2.4}$$

Consider the formal solution for Eq (2.4):

$$f(\psi) = \sum_{i=-m}^{m} b_i \vartheta(\psi)^i. \tag{2.5}$$

Under the restriction that both $b_m \neq 0$ and $b_{-m} \neq 0$ simultaneously, the b_i constants must be determined. Concurrently, the function is generated via the subsequent Backlund transformation.

$$\vartheta(\psi) = \frac{-\tau B + A\phi(\psi)}{A + B\phi(\psi)}. \tag{2.6}$$

With the requirement that $B \neq 0$, let (τ), (A) and (B) be constants. Furthermore, suppose that $\phi(\psi)$ is a function that has the following definition:

$$\frac{d\phi}{d\psi} = \tau + \phi(\psi)^2. \tag{2.7}$$

It is commonly acknowledged that the following are the solutions to Eq (2.7):

$$(i) \quad \text{If} \quad \tau < 0, \quad \text{then} \quad \phi(\psi) = -\sqrt{-\tau}\tanh(\sqrt{-\tau}\psi), \quad \text{or} \quad \phi(\psi) = -\sqrt{-\tau}coth(\sqrt{-\tau}\psi). \tag{2.8}$$

$$(ii) \quad \text{If} \quad \tau > 0, \quad \text{then} \quad \phi(\psi) = \sqrt{\tau}\tan(\sqrt{\tau}\psi), \quad \text{or} \quad \phi(\psi) = -\sqrt{\tau}cot(\sqrt{\tau}\psi). \tag{2.9}$$

$$(iii) \quad \text{If} \quad \tau = 0, \quad \text{then} \quad \phi(\psi) = \frac{-1}{\psi}. \tag{2.10}$$

Under the framework of Eq (2.5), the positive integer (N) can be found by using homogeneous balancing principles, which entail finding equilibrium between the highest order derivatives and the nonlinear variables in Eq (2.4). $f(\psi)$ degree can be expressed more precisely as $D[f(\psi)] = N$. Therefore, this enables us to perform the following computation of the degree of linked expressions:

$$D\left[\frac{d^k f}{d\psi^k}\right] = N + k, \quad D\left[f^J \frac{d^k f}{d\psi^k}\right]^s = NJ + s(k + N). \tag{2.11}$$

Algebraic equations are established by combining Eq (2.4) with Eqs (2.5) and (2.7), grouping terms with the same powers of $f(\psi)$, and then equating them to zero. Applying Maple software to deduce the pertinent values for various parameters will result in an efficient resolution of this system. Thus, this makes it easier to compute the soliton wave-propagating solutions to Eq (2.1) with accuracy by computational analysis.

3. Execution of the problem

Using the approach outlined in Section 2, we methodically solve the fractional EMC equation (1.1), concentrating on solutions for single waves. Using the wave transformation described in Eq (2.3), our analysis is simplified inside the EMC equation framework. We then show the resulting equation, a derived nonlinear ordinary differential equation (ODE), that captures the nonlinear dynamics after this transformation step. This new equation is a concise expression derived from the original fractional partial differential equation (PDE) and represents a breakthrough in our comprehension of the fundamental dynamics in the frictional EMC framework.

$$q^3 f''' + 2\lambda q^2 (f')^2 - \omega f' = 0. \tag{3.1}$$

Equation (3.1) as well as Eqs (2.7) and (2.6) all incorporate the replacement given in Eq (2.5). After collecting coefficients for $\phi^i(\psi)$ in a methodical manner, we create an algebraic system of equations that equals zero. By utilizing the computing power of Maple, we can solve this system of algebraic equations and obtain the following answers. This methodology guarantees a methodical and effective extraction of the solutions, revealing insights into the interrelationships between variables in the specified mathematical context:

Case 1.

$$b_0 = b_0,\ b_1 = b_1,\ b_{-1} = -\frac{A^2 b_1}{B^2},\ q = q,\ \omega = -16\,\frac{A^2 q^3}{B^2},\ \lambda = -3\,\frac{q}{b_1},\ \tau = \frac{A^2}{B^2},\ B = B. \tag{3.2}$$

Case 2.

$$b_0 = b_0,\ b_1 = 0,\ b_{-1} = b_{-1},\ q = 1/3\,\frac{\lambda\, b_{-1}}{\tau},\ \omega = -\frac{4}{27}\,\frac{\lambda^3 {b_{-1}}^3}{\tau^2},\ \lambda = \lambda,\ \tau = \tau,\ B = B. \tag{3.3}$$

Case 3.

$$b_0 = b_0,\ b_1 = b_1,\ b_{-1} = 0,\ q = -1/3\,\lambda\, b_1,\ \omega = \frac{4}{27}\,\lambda^3 {b_1}^3 \tau,\ \lambda = \lambda,\ \tau = \tau,\ B = B. \tag{3.4}$$

The solution set for the values of (ψ) that follow is obtained by assuming Case 1:

$$\psi = \frac{q y^\beta}{\beta} + 16\,\frac{A^2 q^3 t^\alpha}{B^2 \alpha}. \tag{3.5}$$

Solution Set 1: When $\tau < 0$, then Eq (1.1) brings about the resulting single-wave solutions:

$$\begin{aligned} F_1(x,y,t) =& e^{i\psi}\left[-A^2 b_1\left(A - B\sqrt{-\frac{A^2}{B^2}}\tanh\left(\sqrt{-\frac{A^2}{B^2}}\psi\right)\right)B^{-2}\left(-\frac{A^2}{B} - A\sqrt{-\frac{A^2}{B^2}}\tanh\left(\sqrt{-\frac{A^2}{B^2}}\psi\right)\right)^{-1} + b_0\right] \\ &+ e^{i\psi}\left[b_1\left(-\frac{A^2}{B} - A\sqrt{-\frac{A^2}{B^2}}\tanh\left(\sqrt{-\frac{A^2}{B^2}}\psi\right)\right)\left(A - B\sqrt{-\frac{A^2}{B^2}}\tanh\left(\sqrt{-\frac{A^2}{B^2}}\psi\right)\right)^{-1}\right], \end{aligned} \tag{3.6}$$

or

$$F_2(x,y,t) = e^{i\psi}\left[-A^2 b_1\left(A - B\sqrt{-\frac{A^2}{B^2}}\coth\left(\sqrt{-\frac{A^2}{B^2}}\psi\right)\right)B^{-2}\left(-\frac{A^2}{B} - A\sqrt{-\frac{A^2}{B^2}}\coth\left(\sqrt{-\frac{A^2}{B^2}}\psi\right)\right)^{-1} + b_0\right] + e^{i\psi}\left[b_1\left(-\frac{A^2}{B} - A\sqrt{-\frac{A^2}{B^2}}\coth\left(\sqrt{-\frac{A^2}{B^2}}\psi\right)\right)\left(A - B\sqrt{-\frac{A^2}{B^2}}\coth\left(\sqrt{-\frac{A^2}{B^2}}\psi\right)\right)^{-1}\right]. \tag{3.7}$$

Solution Set 2: When $\tau > 0$, then Eq (1.1) brings about the resulting single-wave solutions:

$$F_3(x,y,t) = e^{i\psi}\left[-A^2 b_1\left(A + B\sqrt{\frac{A^2}{B^2}}\tan\left(\sqrt{\frac{A^2}{B^2}}\psi\right)\right)B^{-2}\left(-\frac{A^2}{B} + A\sqrt{\frac{A^2}{B^2}}\tan\left(\sqrt{\frac{A^2}{B^2}}\psi\right)\right)^{-1} + b_0\right] + e^{i\psi}\left[b_1\left(-\frac{A^2}{B} + A\sqrt{\frac{A^2}{B^2}}\tan\left(\sqrt{\frac{A^2}{B^2}}\psi\right)\right)\left(A + B\sqrt{\frac{A^2}{B^2}}\tan\left(\sqrt{\frac{A^2}{B^2}}\psi\right)\right)^{-1}\right], \tag{3.8}$$

or

$$F_4(x,y,t) = e^{i\psi}\left[-A^2 b_1\left(A - B\sqrt{\frac{A^2}{B^2}}\cot\left(\sqrt{\frac{A^2}{B^2}}\psi\right)\right)B^{-2}\left(-\frac{A^2}{B} - A\sqrt{\frac{A^2}{B^2}}\cot\left(\sqrt{\frac{A^2}{B^2}}\psi\right)\right)^{-1} + b_0\right] + e^{i\psi}\left[b_1\left(-\frac{A^2}{B} - A\sqrt{\frac{A^2}{B^2}}\cot\left(\sqrt{\frac{A^2}{B^2}}\psi\right)\right)\left(A - B\sqrt{\frac{A^2}{B^2}}\cot\left(\sqrt{\frac{A^2}{B^2}}\psi\right)\right)^{-1}\right]. \tag{3.9}$$

Solution Set 3: When $\tau = 0$, then Eq (1.1) brings about the resulting single-wave solutions:

$$F_5(x,y,t) = e^{i\psi}\left[-A^2 b_1\left(A - \frac{B}{\psi}\right)B^{-2}\left(-\frac{A^2}{B} - \frac{A}{\psi}\right)^{-1} + b_0 + b_1\left(-\frac{A^2}{B} - \frac{A}{\psi}\right)\left(A - \frac{B}{\psi}\right)^{-1}\right]. \tag{3.10}$$

The solution set for the values of (ψ) that follow is obtained by assuming Case 2:

$$\psi = 1/3\,\frac{\lambda\, b_{-1} y^{\beta}}{\tau\beta} + \frac{4}{27}\,\frac{\lambda^3 {b_{-1}}^3 t^{\alpha}}{\tau^2\alpha}. \tag{3.11}$$

Solution Set 1: When $\tau < 0$, then Eq (1.1) brings about the resulting single-wave solutions:

$$F_6(x,y,t) = e^{i\psi}\left[\frac{b_{-1}\left(A - B\sqrt{-\tau}\tanh\left(\sqrt{-\tau}\psi\right)\right)}{-\tau B - A\sqrt{-\tau}\tanh\left(\sqrt{-\tau}\psi\right)} + b_0\right], \tag{3.12}$$

or

$$F_7(x,y,t) = e^{i\psi}\left[\frac{b_{-1}\left(A - B\sqrt{-\tau}\coth\left(\sqrt{-\tau}\psi\right)\right)}{-\tau B - A\sqrt{-\tau}\coth\left(\sqrt{-\tau}\psi\right)} + b_0\right]. \tag{3.13}$$

Solution Set 2: When $\tau > 0$, then Eq (1.1) brings about the resulting single-wave solutions:

$$F_8(x,y,t) = e^{i\psi}\left[\frac{b_{-1}\left(A + B\sqrt{\tau}\tan\left(\sqrt{\tau}\psi\right)\right)}{-\tau B + A\sqrt{\tau}\tan\left(\sqrt{\tau}\psi\right)} + b_0\right], \tag{3.14}$$

or

$$F_9(x,y,t) = e^{i\psi}\left[\frac{b_{-1}\left(A - B\sqrt{\tau}\cot\left(\sqrt{\tau}\psi\right)\right)}{-\tau B - A\sqrt{\tau}\cot\left(\sqrt{\tau}\psi\right)} + b_0\right]. \tag{3.15}$$

Solution Set 3: When $\tau = 0$, then Eq (1.1) brings about the resulting single-wave solutions:

$$F_{10}(x,y,t) = e^{i\psi}\left[b_{-1}\left(A - \frac{B}{\psi}\right)\left(-\tau B - \frac{A}{\psi}\right)^{-1} + b_0\right]. \tag{3.16}$$

The solution set for the values of (ψ) that follow is obtained by assuming Case 3:

$$\psi = -1/3\,\frac{\lambda\, b_1 y^{\beta}}{\beta} - \frac{4}{27}\,\frac{\lambda^3 {b_1}^3 \tau\, t^{\alpha}}{\alpha}. \tag{3.17}$$

Solution Set 1: When $\tau < 0$, then Eq (1.1) brings about the resulting single-wave solutions:

$$F_{11}(x,y,t) = e^{i\psi}\left[b_0 + \frac{b_1\left(-\tau B - A\sqrt{-\tau}\tanh\left(\sqrt{-\tau}\psi\right)\right)}{A - B\sqrt{-\tau}\tanh\left(\sqrt{-\tau}\psi\right)}\right], \tag{3.18}$$

or

$$F_{12}(x,y,t) = e^{i\psi}\left[b_0 + \frac{b_1\left(-\tau B - A\sqrt{-\tau}\coth\left(\sqrt{-\tau}\psi\right)\right)}{A - B\sqrt{-\tau}\coth\left(\sqrt{-\tau}\psi\right)}\right]. \tag{3.19}$$

Solution Set 2: When $\tau > 0$, then Eq (1.1) brings about the resulting single-wave solutions:

$$F_{13}(x,y,t) = e^{i\psi}\left[b_0 + \frac{b_1\left(-\tau B + A\sqrt{\tau}\tan\left(\sqrt{\tau}\psi\right)\right)}{A + B\sqrt{\tau}\tan\left(\sqrt{\tau}\psi\right)}\right], \tag{3.20}$$

or

$$F_{14}(x,y,t) = e^{i\psi}\left[b_0 + \frac{b_1\left(-\tau B - A\sqrt{\tau}\cot\left(\sqrt{\tau}\psi\right)\right)}{A - B\sqrt{\tau}\cot\left(\sqrt{\tau}\psi\right)}\right]. \tag{3.21}$$

Solution Set 3: When $\tau = 0$, then Eq (1.1) brings about the resulting single-wave solutions:

$$F_{15}(x,y,t) = e^{i\psi}\left[b_0 + b_1\left(-\tau B - \frac{A}{\psi}\right)\left(A - \frac{B}{\psi}\right)^{-1}\right]. \tag{3.22}$$

4. Results and discussion

When used in conjunction with the Backlund transformation, the Riccati-Bernoulli sub-ODE technique becomes a powerful analytical tool for studying complex dynamic systems, including shallow water waves, tsunami modeling, coastal engineering, environmental impact assessment, river and estuary dynamics, and biophysical applications. This method is well-known for its flexibility in a wide range of physical systems and its capacity to produce a large number of periodic and single traveling wave solutions, each with unique properties. Interestingly, this is accomplished without using the discretization and linearization steps that are frequently used in problem-solving techniques. This highlights the Riccati-Bernoulli sub-ODE technique's intrinsic effectiveness and wide applicability as a sophisticated analytical framework in the investigation of complicated dynamic systems.

The results obtained with this approach provide exact solutions for systems representing the physical phenomena outlined above, which contributes to our comprehension of the complex dynamics involved in these processes. The flexibility of the approach is crucial for capturing complex behaviors, yielding a wide range of solutions with different parameters. Moreover, the analytical solutions that are obtained are used as standards, which makes it easier to thoroughly assess accuracy and strengthen stability analyses, which are essential for guaranteeing the dependability of computer models. One notable feature of this approach is its ability to produce self-reinforcing solitary waves with solitons with the least amount of energy loss. Because soliton formation is a complex process resulting from a fine balance between linear and nonlinear mechanisms, it opens up new possibilities for investigating and understanding the dynamics of complex physical systems. The recently found exact solutions to this equation exhibit a high degree of variation compared to the previously reported results in the literature. We visualize these solutions as part of our thorough investigation, and the results show a broad spectrum including shock-type, periodic, kink, and anti-kink structures. Each wave has unique applications and significance. Shock waves are used in fluid dynamics, especially in supersonic flows and explosive events. They are characterized by abrupt and fast changes in the physical properties. Periodic waves can be thought of as steady, recurring perturbations in the domain of solitary waves. Kink waves can be seen in a variety of systems, including some plasma waves. They are characterized by a sudden change in amplitude that frequently has a discernible bend. In contrast, the anti-kink waves imply non-linear optics and plasma physics due to their abrupt amplitude change in the opposite direction.

The graphical discussion delves into the interpretation of the figures presented in the study. Each figure showcases variations in the real and imaginary parts of specific solutions, providing insights into their behavior and characteristics.

Figure 1 illustrates the variations in the real and imaginary parts of the solution $F_1(x, y, t)$, highlighting any oscillatory patterns, amplitude changes, or spatial distribution of the solution. Figure 2 presents similar variations for the solution $F_5(x, y, t)$, allowing for comparisons with Figure 1 and potentially revealing differences in behavior or dynamics. In Figure 3, the focus shifts to the solution $F_{10}(x, y, t)$, offering further insights into its real and imaginary components, potentially uncovering unique features or phenomena. Figure 4 provides additional perspectives on the solution $F_{11}(x, y, t)$, enabling a comprehensive analysis of its behavior and interaction with the underlying system dynamics. Finally, Figure 5 offers insights into the solution $F_{15}(x, y, t)$,

potentially highlighting any distinct characteristics or noteworthy phenomena compared to the previous solutions.

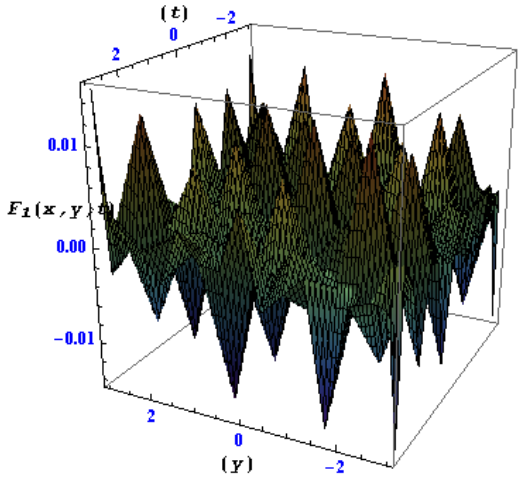

(a) A three-dimensional plot depicting the multiple singular kinks of the real part of $F_1(x, y, t)$ is presented.

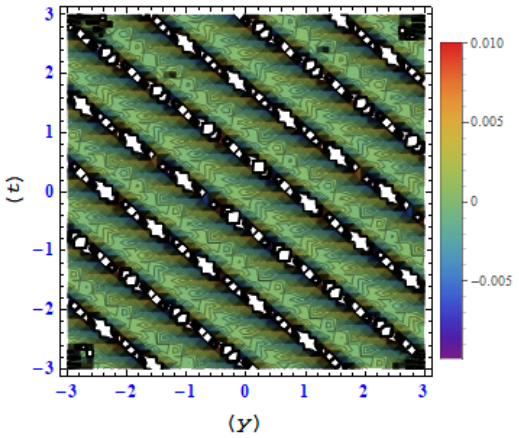

(b) A contour plot representing the real part of $F_1(x, y, t)$ is depicted.

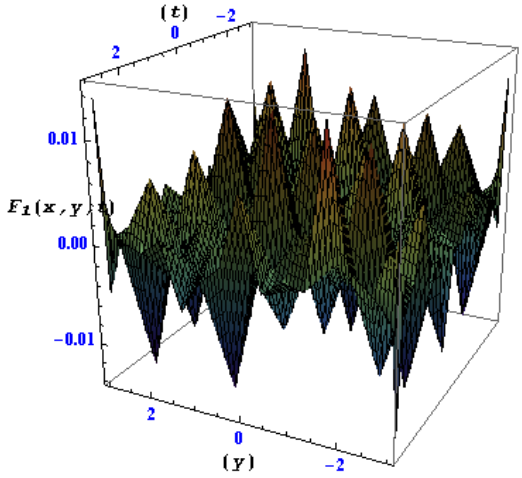

(c) A three-dimensional plot depicting the multiple singular kinks of the imaginary part of $F_1(x, y, t)$ is presented.

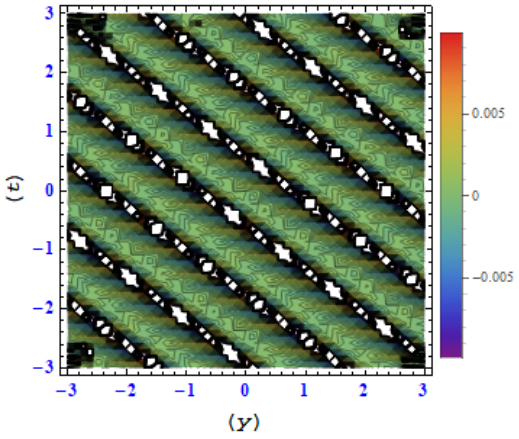

(d) A contour plot representing the imaginary part of $F_1(x, y, t)$ is depicted.

Figure 1. In these graphical representations, variations are shown for the real and imaginary parts of the solution $F_1(x, y, t)$.

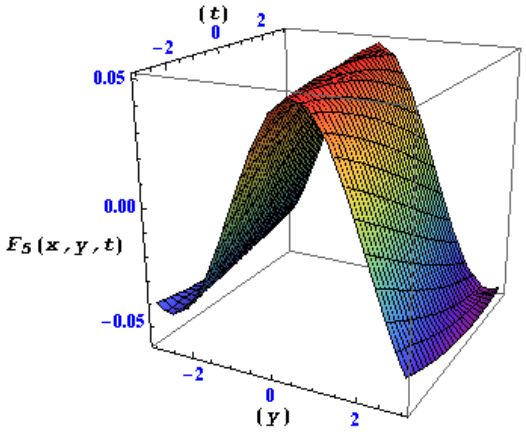

(a) A three-dimensional plot depicting the periodic wave of the real part of $F_5(x, y, t)$ is presented.

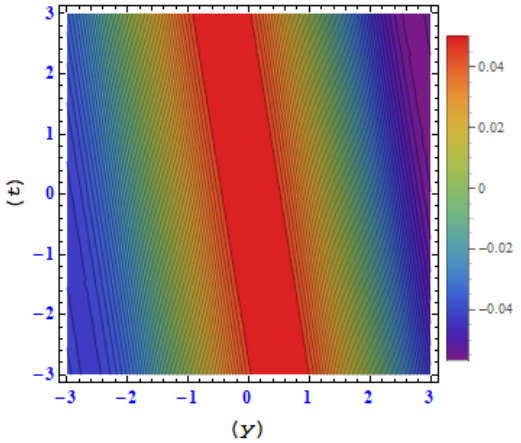

(b) A contour plot representing the real part of $F_5(x, y, t)$ is depicted.

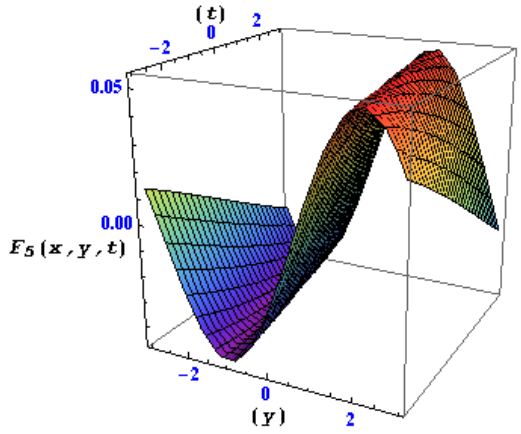

(c) A three-dimensional plot depicting the periodic wave of the imaginary part of $F_5(x, y, t)$ is presented.

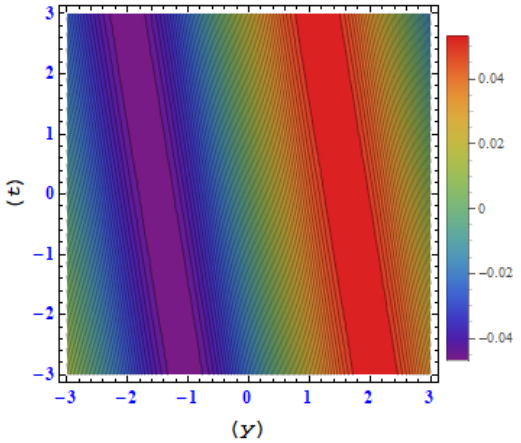

(d) A contour plot representing the imaginary part of $F_5(x, y, t)$ is depicted.

Figure 2. In these graphical representations, variations are shown for the real and imaginary parts of the solution $F_5(x, y, t)$.

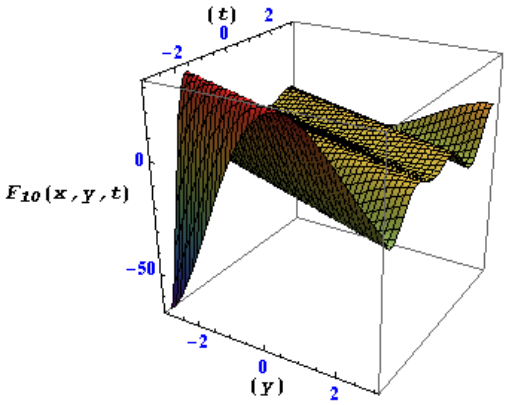

(a) A three-dimensional plot depicting the bifurcating periodic wave of the real part of $F_{10}(x, y, t)$ is presented.

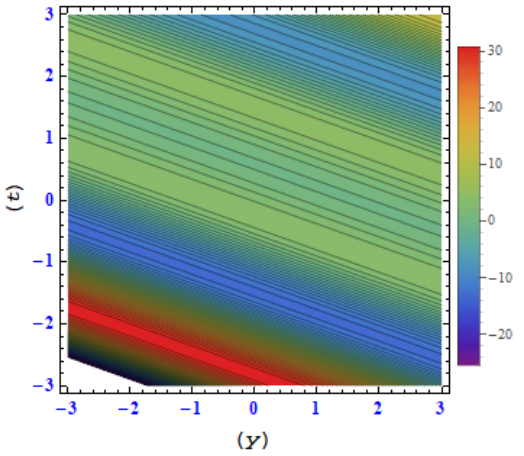

(b) A contour plot representing the real part of $F_{10}(x, y, t)$ is depicted.

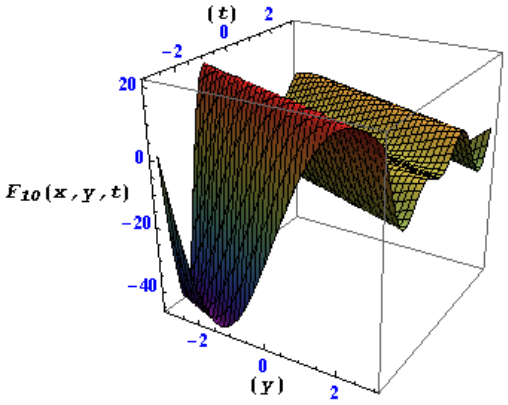

(c) A three-dimensional plot depicting the bifurcating periodic wave of the imaginary part of $F_{10}(x, y, t)$ is presented.

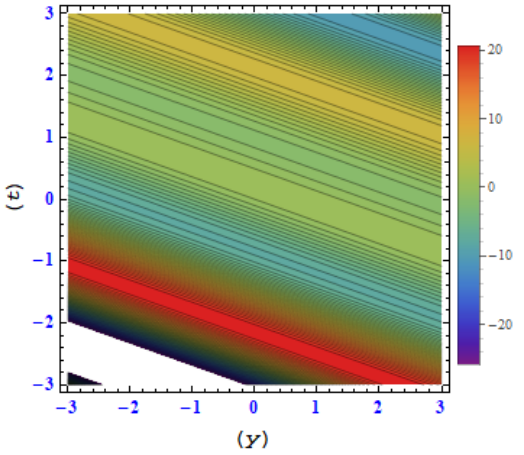

(d) A contour plot representing the imaginary part of $F_{10}(x, y, t)$ is depicted.

Figure 3. In these graphical representations, variations are shown for the real and imaginary parts of the solution $F_{10}(x, y, t)$.

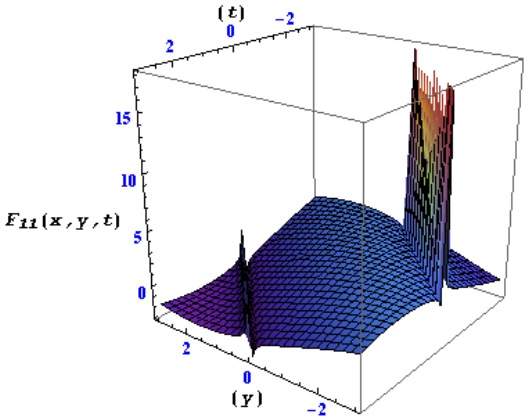

(a) A three-dimensional plot depicting the bright soliton of the real part of $F_{11}(x, y, t)$ is presented.

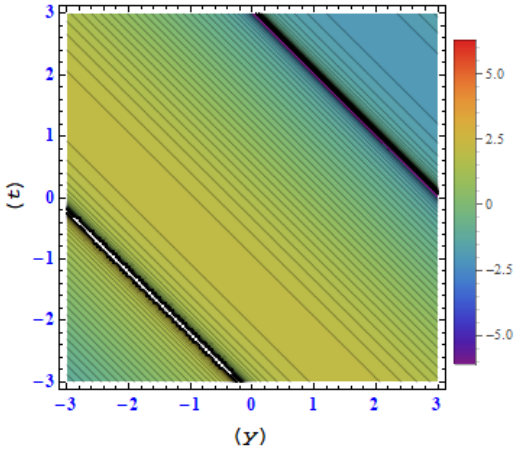

(b) A contour plot representing the real part of $F_{11}(x, y, t)$ is depicted.

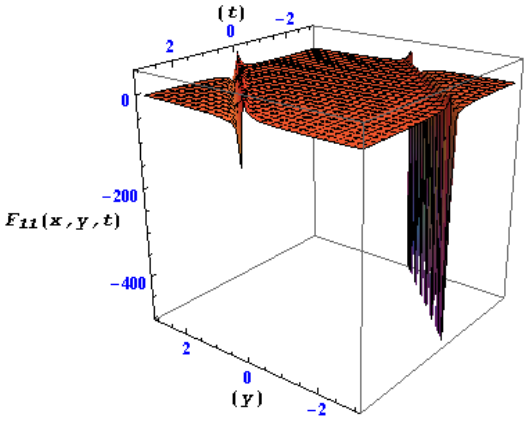

(c) A three-dimensional plot depicting the dark soliton of imaginary part of $F_{11}(x, y, t)$ is presented.

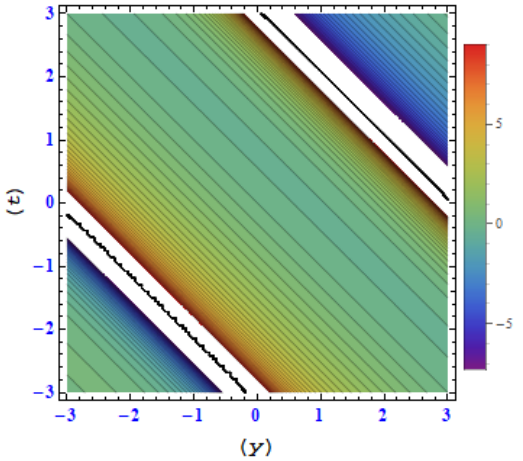

(d) A contour plot representing the imaginary part of $F_{11}(x, y, t)$ is depicted.

Figure 4. In these graphical representations, variations are shown for the real and imaginary parts of the solution $F_{11}(x, y, t)$.

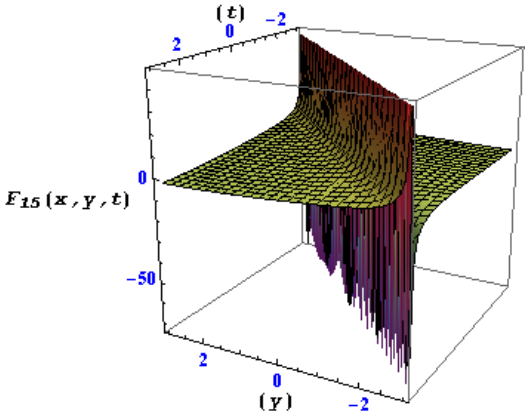

(a) A three-dimensional plot depicting the cuspon kink of the real part of $F_{15}(x, y, t)$ is presented.

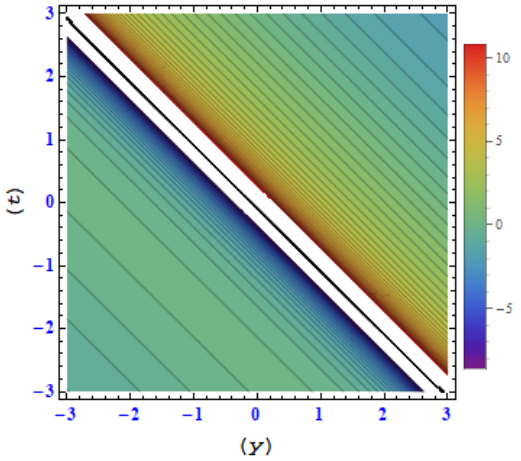

(b) A contour plot representing the real part of $F_{15}(x, y, t)$ is depicted.

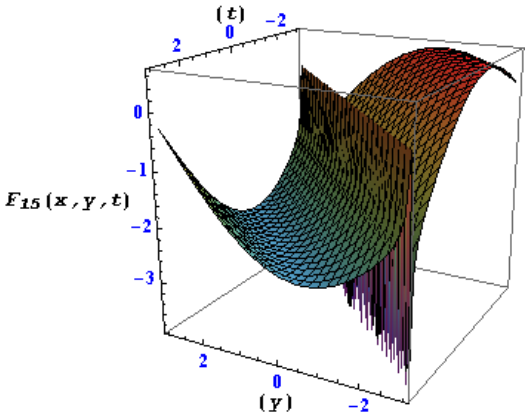

(c) A three-dimensional plot depicting the bifurcated wave of imaginary part of $F_{15}(x, y, t)$ is presented.

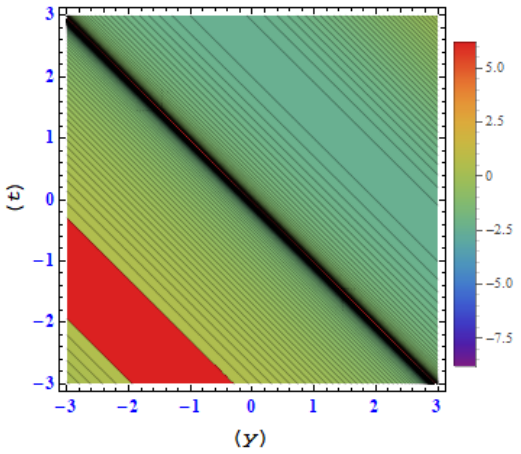

(d) A contour plot representing the imaginary part of $F_{15}(x, y, t)$ is depicted.

Figure 5. In these graphical representations, variations are shown for the real and imaginary parts of the solution $F_{15}(x, y, t)$.

In Table 1, comparison of the current approach with the alternative approaches, the simple equation approach [4] and G'/G-expansion method [9]. Through a detailed examination of these graphical representations, the study aims to enhance understanding of the soliton solutions within the context of the investigated equations, providing valuable insights for further analysis and interpretation.

Table 1. Comparison of the current approach with the alternative approaches, the simple equation approach [4] and G'/G-expansion method [9].

Case I: $\tau < 0$ Present method
$u = e^{i\psi}\left[-A^2 b_1\left(A - B\sqrt{-\frac{A^2}{B^2}}\tanh\left(\sqrt{-\frac{A^2}{B^2}}\psi\right)\right)B^{-2}\left(-\frac{A^2}{B} - A\sqrt{-\frac{A^2}{B^2}}\tanh\left(\sqrt{-\frac{A^2}{B^2}}\psi\right)\right)^{-1} + b_0\right]$ $+ e^{i\psi}\left[b_1\left(-\frac{A^2}{B} - A\sqrt{-\frac{A^2}{B^2}}\tanh\left(\sqrt{-\frac{A^2}{B^2}}\psi\right)\right)\left(A - B\sqrt{-\frac{A^2}{B^2}}\tanh\left(\sqrt{-\frac{A^2}{B^2}}\psi\right)\right)^{-1}\right]$
Case I: $\lambda^2 - 4\mu < 0$ G'/G-expansion method
$u = \frac{6/}{\beta}\left[\frac{-\lambda}{2} + \vartheta_2\left(\frac{-c_1\sin(\vartheta_2\zeta)+c_2\cos(\vartheta_2\zeta)}{c_1\cos(\vartheta_2\zeta)+c_2\sin(\vartheta_2\zeta)}\right)\right]$
Case I: $\mu > 0,\ \eta < 0$ Simple equation method
$u = a_0 - \frac{6/\eta}{\delta}\left(\frac{\mu e^{\mu(\psi+\psi_0)}}{1-\eta e^{\mu(\psi+\psi_0)}}\right)$
Case II: $\tau > 0$ Present method
$u = e^{i\psi}\left[-A^2 b_1\left(A + B\sqrt{\frac{A^2}{B^2}}\tan\left(\sqrt{\frac{A^2}{B^2}}\psi\right)\right)B^{-2}\left(-\frac{A^2}{B} + A\sqrt{\frac{A^2}{B^2}}\tan\left(\sqrt{\frac{A^2}{B^2}}\psi\right)\right)^{-1} + b_0\right]$ $e^{i\psi}\left[b_1\left(-\frac{A^2}{B} + A\sqrt{\frac{A^2}{B^2}}\tan\left(\sqrt{\frac{A^2}{B^2}}\psi\right)\right)\left(A + B\sqrt{\frac{A^2}{B^2}}\tan\left(\sqrt{\frac{A^2}{B^2}}\psi\right)\right)^{-1}\right]$
Case II: $\lambda^2 - 4\mu > 0$ G'/G-expansion method
$u = \frac{6l}{\beta}\left[\frac{-\lambda}{2} + \vartheta_1\left(\frac{c_1\sinh(\vartheta_1\zeta)+c_2\cosh(\vartheta_1\zeta)}{c_1\cosh(\vartheta_1\zeta)+c_2\sinh(\vartheta_1\zeta)}\right)\right]$
Case II: $\mu < 0,\ \eta > 0$ Simple equation method
$u = a_0 + \frac{6/\eta}{\delta}\left(\frac{\mu e^{\mu(\psi+\psi_0)}}{1+\eta e^{\mu(\psi+\psi_0)}}\right)$ where $\psi = \frac{kx^\alpha}{\Gamma(\alpha+1)} + \frac{ly^\alpha}{\Gamma(\alpha+1)} - \frac{\beta\mu^2 t^\alpha}{\Gamma(\alpha+1)}$
Case III: $\tau = 0$ Present method
$u = e^{i\psi}\left[-A^2 b_1\left(A - \frac{B}{\psi}\right)B^{-2}\left(-\frac{A^2}{B} - \frac{A}{\psi}\right)^{-1} + b_0 + b_1\left(-\frac{A^2}{B} - \frac{A}{\psi}\right)\left(A - \frac{B}{\psi}\right)^{-1}\right]$
Case III: $\lambda^2 - 4\mu = c = 0$ G'/G-expansion method
$u = a_0 + \frac{6l}{\beta}\left(\frac{-\lambda}{2} + \frac{c_2}{c_1+c_2\zeta}\right)$ where $\zeta = \frac{kx^\alpha}{\Gamma(\alpha+1)} + \frac{ly^\alpha}{\Gamma(\alpha+1)} - \frac{ct^\alpha}{\Gamma(\alpha+1)}$ and $\vartheta_1 = \frac{\sqrt{c/\beta^3}}{2},\ \vartheta_2 = \frac{\sqrt{-c/l^3}}{2}$

5. Conclusions

Through the use of Backlund transformation techniques, we have improved the application of the Riccati Bernoulli sub-ODE method in this work. The fractional EMC equation stable solitary wave solutions have been successfully derived using this extension. The results validate the flexibility of

our suggested method, which may now be used to solve a larger class of nonlinear evolution equations. Future research avenues and intriguing applications can be pursued with the kink, anti-kink, and periodic solutions obtained by using our proposed approach. These results have the potential to improve the communications systems by employing solitary wave stability for long-distance transmission. Investigating the behavior of kink, anti-kink, and periodic solutions provides important insights for manipulating nonlinear optical phenomena and creating cutting-edge optical devices in the fields of material sciences and non-linear optics. Moreover, energy transmission in periodic structures can be studied using periodic solutions, which might advance knowledge of energy propagation and possibly enhance energy harvesting technology. Our analysis demonstrates the effectiveness of the technique, establishing it as a useful resource for theoretical physicists and mathematicians, especially when dealing with discrete nonlinear dynamics. Systems that can be solved analytically or that admit explicit solutions are given preference. This work is important not only for theoretical biologists looking for insights into physical applications but also for fluid dynamics engineers.

Use of AI tools declaration

The authors declare they have not used Artificial Intelligence (AI) tools in the creation of this article.

Funding

This work was supported by the Deanship of Scientific Research, Vice Presidency for Graduate Studies and Scientific Research, King Faisal University, Saudi Arabia (Grant No. 6158).

Acknowledgments

This work was supported by the Deanship of Scientific Research, Vice Presidency for Graduate Studies and Scientific Research, King Faisal University, Saudi Arabia (Grant No. 6158).

Conflict of interest

The authors declare that they have no conflicts of interest.

References

1. M. M. A. Khater, Multi-vector with nonlocal and non-singular kernel ultrashort optical solitons pulses waves in birefringent fibers, *Chaos Solitons Fract.*, **167** (2023), 113098. https://doi.org/10.1016/j.chaos.2022.113098
2. M. M. A. Khater, Novel computational simulation of the propagation of pulses in optical fibers regarding the dispersion effect, *Int. J. Modern Phys. B*, **37** (2023), 2350083. https://doi.org/10.1142/S0217979223500832

3. M. M. A. Khater, Prorogation of waves in shallow water through unidirectional Dullin-Gottwald-Holm model; computational simulations, *Int. J. Modern Phys. B*, **37** (2023), 2350071. https://doi.org/10.1142/S0217979223500716
4. S. Phoosree, W. Thadee, Wave effects of the fractional shallow water equation and the fractional optical fiber equation, *Front. Appl. Math. Stat.*, **8** (2022), 900369. https://doi.org/10.3389/fams.2022.900369
5. M. M. Bhatti, D. Q. Lu, An application of Nwogu's Boussinesq model to analyze the head-on collision process between hydroelastic solitary waves, *Open Phys.*, **17** (2019), 177–191. https://doi.org/ 10.1515/phys-2019-0018
6. A. A. Gaber, A. F. Aljohani, A. Ebaid, J. T. Machado, The generalized Kudryashov method for nonlinear space-time fractional partial differential equations of Burgers type, *Nonlinear Dyn.*, **95** (2019), 361–368. https://doi.org/10.1007/s11071-018-4568-4
7. M. H. Hao, Y. N. Zhang, J. Pang, Solving fractional nonlinear partial differential equations by the modified Kudryashov method, *J. Phys. Conf. Ser.*, **1300** (2019), 012059. https://doi.org/10.1088/1742-6596/1300/1/012059
8. H. Yepez-Martinez, J. F. Gomez-Aguilar, Fractional sub-equation method for Hirota-Satsuma-coupled KdV equation and coupled mKdV equation using the Atangana's conformable derivative, *Waves Random Complex Media*, **29** (2019), 678–693. https://doi.org/10.1080/17455030.2018.1464233
9. S. Phoosree, S. Chinviriyasit, New analytic solutions of some fourth-order nonlinear space-time fractional partial differential equations by G'/G-expansion method, *Songklanakarin J. Sci. Technol.*, **43** (2021), 795–801.
10. H. Yasmin, N. H. Aljahdaly, A. M. Saeed, R. Shah, Investigating symmetric soliton solutions for the fractional coupled Konno-Onno system using improved versions of a novel analytical technique, *Mathematics*, **11** (2023), 1–30. https://doi.org/10.3390/math11122686
11. A. Shafee, Y. Alkhezi, R. Shah, Efficient solution of fractional system partial differential equations using Laplace residual power series method, *Fractal Fract.*, **7** (2023), 1–12. https://doi.org/10.3390/fractalfract7060429
12. T. Y. Han, Z. B. Zhao, K. Zhang, C. Tang, Chaotic behavior and solitary wave solutions of stochastic-fractional Drinfel'd-Sokolov-Wilson equations with Brownian motion, *Results Phys.*, **51** (2023), 106657. https://doi.org/10.1016/j.rinp.2023.106657
13. A. H. Arnous, M. Mirzazadeh, L. Akinyemi, A. Akbulut, New solitary waves and exact solutions for the fifth-order nonlinear wave equation using two integration techniques, *J. Ocean Eng. Sci.*, **8** (2023), 475–480. https://doi.org/10.1016/j.joes.2022.02.012
14. A. H. Arnous, M. Mirzazadeh, A. Akbulut, L. Akinyemi, Optical solutions and conservation laws of the Chen-Lee-Liu equation with Kudryashov's refractive index via two integrable techniques, *Waves Random Complex Media*, 2022, 1–17. https://doi.org/ 10.1080/17455030.2022.2045044
15. M. Iqbal, A. R. Seadawy, D. C. Lu, Construction of solitary wave solutions to the nonlinear modified Kortewege-de Vries dynamical equation in unmagnetized plasma via mathematical methods, *Modern Phys. Lett. A*, **33** (2018), 1850183. https://doi.org/ 10.1142/S0217732318501833

16. M. Iqbal, A. R. Seadawy, O. H. Khalil, D. C. Lu, Propagation of long internal waves in density stratified ocean for the (2+1)-dimensional nonlinear Nizhnik-Novikov-Vesselov dynamical equation, *Results Phys.*, **16** (2020), 102838. https://doi.org/10.1016/j.rinp.2019.102838
17. M. Iqbal, A. R. Seadawy, D. C. Lu, Dispersive solitary wave solutions of nonlinear further modified Korteweg-de Vries dynamical equation in an unmagnetized dusty plasma, *Modern Phys. Lett. A*, **33** (2018), 1850217. https://doi.org/10.1142/S0217732318502176
18. M. Iqbal, A. R. Seadawy, D. C. Lu, Applications of nonlinear longitudinal wave equation in a magneto-electro-elastic circular rod and new solitary wave solutions, *Modern Phys. Lett. B*, **33** (2019), 1950210. https://doi.org/10.1142/S0217984919502105
19. A. R. Seadawy, M. Iqbal, D. C. Lu, Applications of propagation of long-wave with dissipation and dispersion in nonlinear media via solitary wave solutions of generalized Kadomtsev-Petviashvili modified equal width dynamical equation, *Comput. Math. Appl.*, **78** (2019), 3620–3632. https://doi.org/10.1016/j.camwa.2019.06.013
20. A. A. Alderremy, R. Shah, N. Iqbal, S. Aly, K. Nonlaopon, Fractional series solution construction for nonlinear fractional reaction-diffusion Brusselator model utilizing Laplace residual power series, *Symmetry*, **14** (2022), 1–20. https://doi.org/10.3390/sym14091944
21. H. M. Srivastava, R. Shah, H. Khan, M. Arif, Some analytical and numerical investigation of a family of fractional-order Helmholtz equations in two space dimensions, *Math. Methods Appl. Sci.*, **43** (2020), 199–212. https://doi.org/10.1002/mma.5846
22. A. S. Alshehry, M. Imran, A. Khan, R. Shah, W. Weera, Fractional view analysis of Kuramoto-Sivashinsky equations with non-singular kernel operators, *Symmetry*, **14** (2022), 1–24. https://doi.org/10.3390/sym14071463
23. S. Mukhtar, R. Shah, S. Noor, The numerical investigation of a fractional-order multi-dimensional model of Navier-Stokes equation via novel techniques, *Symmetry*, **14** (2022), 1–21. https://doi.org/10.3390/sym14061102
24. M. Naeem, O. F. Azhar, A. M. Zidan, K. Nonlaopon, R. Shah, Numerical analysis of fractional-order parabolic equations via Elzaki transform, *J. Funct. Spaces*, **2021** (2021), 1–10. https://doi.org/10.1155/2021/3484482
25. S. S. Ray, R. K. Bera, Analytical solution of a fractional diffusion equation by Adomian decomposition method, *Appl. Math. Comput.*, **174** (2006), 329–336. https://doi.org/10.1016/j.amc.2005.04.082
26. B. K. Singh, P. Kumar, Fractional variational iteration method for solving fractional partial differential equations with proportional delay, *Int. J. Differ. Equ.*, **2017** (2017), 1–11. https://doi.org/10.1155/2017/5206380
27. S. Noor, A. S. Alshehry, A. Shafee, R. Shah, Families of propagating soliton solutions for (3+1)-fractional Wazwaz-BenjaminBona-Mahony equation through a novel modification of modified extended direct algebraic method, *Phys. Scr.*, **99** (2024), 045230. https://doi.org/10.1088/1402-4896/ad23b0
28. H. Yasmin, A. S. Alshehry, A. H. Ganie, A. M. Mahnashi, R. Shah, Perturbed Gerdjikov-Ivanov equation: soliton solutions via Backlund transformation, *Optik*, **298** (2024), 171576. https://doi.org/10.1016/j.ijleo.2023.171576

29. S. Alshammari, K. Moaddy, R. Shah, M. Alshammari, Z. Alsheekhhussain, M. M. Al-Sawalha, et al., Analysis of solitary wave solutions in the fractional-order Kundu-Eckhaus system, *Sci. Reports*, **14** (2024), 3688. https://doi.org/10.1038/s41598-024-53330-7

30. Z. Alsheekhhussain, K. Moaddy, R. Shah, S. Alshammari, M. Alshammari, M. M. Al-Sawalha, et al., Extension of the optimal auxiliary function method to solve the system of a fractional-order Whitham-Broer-Kaup equation, *Fractal Fract.*, **8** (2024), 1–14. https://doi.org/10.3390/fractalfract8010001

31. M. M. Al-Sawalha, S. Mukhtar, R. Shah, A. H. Ganie, K. Moaddy, Solitary waves propagation analysis in nonlinear dynamical system of fractional coupled Boussinesq-Whitham-Broer-Kaup equation, *Fractal Fract.*, **7** (2023), 1–26. https://doi.org/10.3390/fractalfract7120889

32. M. Alqhtani, K. M. Saad, R. Shah, W. M. Hamanah, Discovering novel soliton solutions for (3+1)-modified fractional Zakharov-Kuznetsov equation in electrical engineering through an analytical approach, *Opt. Quant. Electron.*, **55** (2023), 1149. https://doi.org/10.1007/s11082-023-05407-2

33. H. Yasmin, N. H. Aljahdaly, A. M. Saeed, R. Shah, Probing families of optical soliton solutions in fractional perturbed Radhakrishnan-Kundu-Lakshmanan model with improved versions of extended direct algebraic method, *Fractal Fract.*, **7** (2023), 1–29. https://doi.org/10.3390/fractalfract7070512

34. M. A. E. Abdelrahman, M. A. Sohaly, Solitary waves for the modified Korteweg-de Vries equation in deterministic case and random case, *J. Phys. Math.*, **8** (2017), 1–6.

35. M. A. E. Abdelrahman, M. A. Sohaly, Solitary waves for the nonlinear Schrodinger problem with the probability distribution function in the stochastic input case, *Eur. Phys. J. Plus*, **132** (2017), 339. https://doi.org/10.1140/epjp/i2017-11607-5

36. X. F. Yang, Z. C. Deng, Y. Wei, A Riccati-Bernoulli sub-ODE method for nonlinear partial differential equations and its application, *Adv. Differ. Equ.*, **2015** (2015), 1–17.

37. H. K. Barman, M. E. Islam, M. A. Akbar, A study on the compatibility of the generalized Kudryashov method to determine wave solutions, *Propuls. Power Res.*, **10** (2021), 95–105. https://doi.org/10.1016/j.jppr.2020.12.001

38. Z. Y. Yan, Abundant symmetries and exact compacton-like structures in the two-parameter family of the Estevez-Mansfield-Clarkson equations, *Commun. Theor. Phys.*, **37** (2002), 27. https://doi.org/10.1088/0253-6102/37/1/27

39. P. R. Kundu, M. R. A. Fahim, M. E. Islam, M. A. Akbar, The sine-Gordon expansion method for higher-dimensional NLEEs and parametric analysis, *Heliyon*, **7** (2021), E06459. https://doi.org/10.1016/j.heliyon.2021.e06459

40. M. Z. Sarikaya, H. Budak, F. Usta, On generalized the conformable fractional calculus, *TWMS J. Appl. Eng. Math.*, **9** (2019), 792–799.